Colburn ‘j’ factor analysis for offset strip fins in compact heat exchangers

Tanish Samanta[1,a], Gokula Krishna Tavva[1,b], and Chennu Ranganayakulu[1,c]

1 Department of Mechanical Engineering, BITS Pilani, Pilani Campus, Rajasthan 333031, India,

[a] samantanish@gmail.com

[b] gktavva@gmail.com

[c] c.ranganayakulu@pilani.bits-pilani.ac.in

Abstract. Compact heat exchangers frequently utilize offset strip fins to enhance thermal performance in constrained volumes, relying on repeated boundary layer disruption and flow mixing to achieve high convective heat transfer. This paper presents a focused numerical investigation on the *j* factor, aiming to derive correlations that account for variations in key geometric parameters such as lance length (*l*), fin height (*h*), fin thickness (*t*), and fin spacing (*s*). Numerical simulations using computational fluid dynamics were conducted across a broad range of Reynolds numbers spanning laminar, transitional, and turbulent regimes on ANSYS Fluent 2024. Using insights from the data, we derive continuous correlation expressions for *j* in terms of Reynolds number, *Re* and dimensionless geometric parameters. The resulting generalized Colburn *j* factor correlations are applicable across both laminar flow ($300 \leq Re \leq 1500$) and turbulent flow ($2000 \leq Re \leq 6000$) regimes with air being used as the fluid medium and provide a unified predictive model for Offset Strip Fin (OSF) performance in both flow regimes. These correlations offer improved predictive accuracy and serve as robust tools for optimizing compact heat exchanger performance across the practical range of commercially manufactured OSFs. The impact of pressure drop, while acknowledged as critical to overall design, is not addressed in this paper and will be explored in future work.

Keywords: Compact Heat Exchangers, Offset Strip Fins, Colburn *j* factor, ANSYS Fluent.

1 Introduction

Compact heat exchangers (CHEs) enable high heat-transfer rates in minimal volume and weight, making them indispensable across aerospace, automotive, cryogenic and power-generation applications. Among plate-fin CHEs, OSFs are especially effective on the air side because their interrupted, staggered fin layout repeatedly breaks the boundary layer and promotes mixing between core and wall-adjacent flow, producing much higher convective coefficients than continuous fins. Early theoretical and engineering discussions underscored the value of surface interruption and staged flow disruption for compact exchanger performance. Voronin and Dubrovsky [1] highlighted these design principles in foundational work on compact heat-exchange construction and effectiveness.

Extensive experimental databases assembled in the mid-to-late 20th century remain the backbone of OSF sizing and design. Kays and London [2] provided broad experimental coverage of many plate-fin geometries that still guide preliminary design. Wieting [3] subsequently reported empirical j and f correlations for numerous rectangular OSF geometries, but those power-law fits were limited by the ranges and steadiness of the tested flows and do not fully capture transitional behavior. Building on prior measurements, Manglik and Bergles [4] consolidated disparate datasets and proposed unified, continuous j and f for rectangular OSFs spanning laminar through turbulent regimes which proved an important step toward generalizable design relations.

Subsequent experimental and numerical studies have probed flow physics and broadened the design space. Joshi and Webb [5] documented multiple distinct flow regimes in interrupted-fin arrays from steady laminar through oscillatory wakes and periodic vortex shedding to fully turbulent flow and emphasized that transition phenomena complicate single-form correlations. Two-dimensional numerical investigations by Patankar and Prakash [6] exposed detailed recirculation and periodic boundary-layer behavior introduced by fin interruptions, demonstrating enhanced transport even under otherwise laminar conditions. More recent parametric studies examined geometric sensitivities: Dong et al. [7] varied fin spacing and supplied new empirical j, Song et al. [8] showed that omitting offset-ratio effects can lead to large j factor errors, motivating geometry-aware correlations, and Ranganayakulu and Paturu [9] used CFD to quantify how dimensional ratios shift heat-transfer and friction behavior.

Contemporary work continues to expand practical and numerical treatments of CHE performance. Ranganayakulu and Seetharamu [10] provided a modern synthesis of design, analysis and optimization tools (FEM/CFD) for compact exchangers, stressing realistic geometry and model fidelity. Kim et al. [11] offered targeted correlations and optimization results for OSF geometries, while very recent CFD studies such as Aujla and Ranganayakulu [12] have extended correlation work to new fin types and manufacturing-enabled topologies. Together these efforts show steady progress but also reveal persistent gaps: many correlations were developed for limited geometry sets, and the transitional Reynolds-number range where unsteady wakes and three-dimensional interactions arise remains difficult to predict reliably.

Motivated by these gaps, the present study uses validated CFD to explore OSF performance across a wide Reynolds-number range while systematically varying key nondimensional geometry parameters across the fin manufacturing limits for aerospace applications as discussed in Kays and London [2]. Numerical results are benchmarked against established experiments and prior correlations, then used to develop generalized continuous j factor correlations as functions of Re and relevant geometry ratios. The goal is a compact, geometry-aware correlation set that better captures the physics of the entire flow regime and extends design applicability beyond the parameter windows of earlier empirical fits. Foundational CFD guidance and best practices from Anderson [13] inform our modelling approach.

2 Methodology

2.1 Geometry

The offset strip fin geometry under study is illustrated schematically in Fig. 1. These show the primary geometric parameters of an OSF: lance length (l), height (h), thickness (t), and spacing (s). The combination of these parameters defines the fin surface area density and flow passage geometry, which in turn govern heat transfer and friction characteristics.

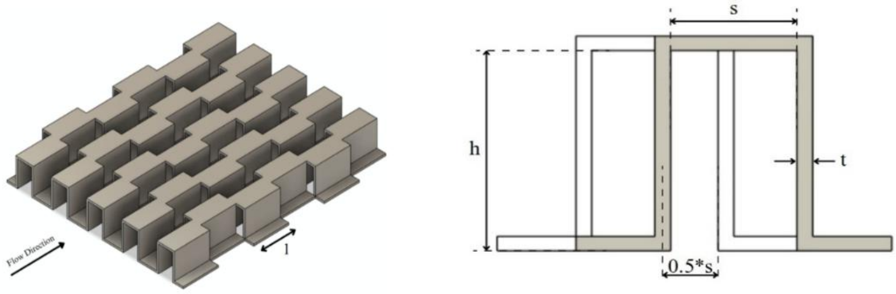

(a) (b)

Fig. 1. Geometric parameters of Offset Strip Fin. (a) Isometric view of OSF array, lance length (l); (b) Cross-sectional view, fin height (h), fin thickness (t), fin spacing (s).

For validation and comparison, a baseline geometry was selected from Kays and London's [2] widely accepted database on compact heat exchanger surfaces. This configuration corresponds to a surface with the following geometric specifications mentioned in Table 1:

Table 1. Geometric parameters used for computational study.

Parameter	For validation	For numerical study	Unit
Plate Spacing (h)	6.35	5.08, 6.35, and 4.52	mm
Fin Thickness (t)	0.102	0.051, 0.102, and 0.254	mm
Fin Length (l)	3.175	2.54, 3.175, and 4.52	mm
Fin Density	15.61	13.95, 15.61, and 19.86	fins/in
Fin Spacing (s)	1.525	$\frac{25.4}{Fin\ Density} - t$	mm

A total of 1,053 CFD simulations were conducted across 81 fin geometries and 13 Reynolds numbers to assess the thermal–hydraulic performance of offset-strip fin arrays. A parametric study varied four key fin dimensions, guided by manufacturing constraints, practical spacing limits, and literature or catalog references, as detailed in Table 1.

2.2 Empirical Relations for *j*

The Colburn *j* factor is defined as:

$$j = St.Pr^{\frac{2}{3}} \tag{1}$$

Here, St is the Stanton number and *Pr* is the Prandtl number. Stanton number is also a function of Prandtl number, Nusselt number and Reynold number which is given by:

$$St = \frac{Nu}{Pr.Re} \tag{2}$$

$$\mathrm{Pr} = \frac{\mu c_p}{\kappa} \tag{3}$$

Where μ is the dynamic viscosity of the fluid and C_p is the specific heat capacity at a constant pressure of the fluid and k is the thermal conductivity of the fluid. The Colburn *j* factor equation established by Kim et al. [11] is taken as reference for the numerical study, which is given below:

$$j = \frac{D_h}{4L} Pr^{\frac{2}{3}} \ln\left(\frac{T_w - T_{in}}{T_w - T_{out}}\right) \tag{4}$$

2.3 Governing Equations

As mentioned in Kim et al. [11] the standard governing equations are:

$$\frac{\partial}{\partial t}(\rho\emptyset) + \frac{\partial}{\partial x_i}(\rho u_i \emptyset) = \frac{\partial}{\partial x_i}\left(\Gamma_\emptyset \frac{\partial \emptyset}{\partial x_i}\right) + S_\emptyset \tag{5}$$

Here, $\Gamma_\emptyset$ and $S_\emptyset$ in the general transport equation are given below in Table 2:

Equation	**∅**	$\boldsymbol{\Gamma_\emptyset}$	$\boldsymbol{S_\emptyset}$
Continuity	1	0	0
u-Momentum	*u*	$\mu + \mu_t$	$-\frac{\partial p}{\partial x}$
v-Momentum	*v*	$\mu + \mu_t$	$-\frac{\partial p}{\partial y}$
w-Momentum	*w*	$\mu + \mu_t$	$-\frac{\partial p}{\partial z}$
Energy	T	$\frac{\mu}{Pr} + \frac{\mu_t}{Pr_t}$	$S_T = \frac{1}{C_p}(\mu\Phi + \rho\varepsilon)$
k	k	$\mu + \frac{\mu_t}{\sigma_k}$	$G_k - \rho\varepsilon$ ($k - \varepsilon$ equation) $G_k - \rho\beta^* k\omega$ ($k - \omega$ equation)
ε	ε	$\mu + \frac{\mu_t}{\sigma_\varepsilon}$	$C_1 G_k \frac{\varepsilon}{k} - C_2(\rho\varepsilon)\frac{\varepsilon}{k}$ (standard) $-C_2(\rho\varepsilon)\frac{\varepsilon}{k + \sqrt{\nu\varepsilon}}$ (realizable)
ω	ω	$\mu + \frac{\mu_t}{\sigma_\omega}$	$\frac{\alpha}{\nu_t} G_k - \rho\beta^*\omega^2 + 2(1 - F_1)\rho\sigma_{\omega,2}\frac{1}{\omega}\frac{\partial k}{\partial x_j}\frac{\partial \omega}{\partial x_j}$

Table 2. Geometric parameters used for validation of computational study.

The flow is treated as steady, incompressible, and Newtonian. The continuity and Navier–Stokes equations, along with the energy equation, were solved with no body forces. Fluid properties were evaluated at the inlet temperature of 300 K. The study considered 6 different RANS turbulence models such as Standard *k-ε* (standard, scalable, and enhanced wall function), Realizable *k-ε* (standard wall function), Standard *k–ω*, and SST *k–ω*, which were used to simulate fluid flow through the baseline fin geometry described in Table 1. The k–ω SST model exhibited the lowest mean absolute percentage error of 6.715% when compared to Kays and London [2] data. As reported in Aujla and Ranganayakulu [12], the incorporation of blending functions F has proven highly accurate results.

2.4 Computational Method

A representative periodic unit cell of the OSF geometry was used as the CFD domain as shown in Fig. 2(a). The side walls and bounding top/bottom planes were treated as symmetry boundaries, and a single module was modelled with periodic boundary conditions in the streamwise direction to reduce the computational effort. A uniform velocity inlet was specified at the entry and a zero-gauge pressure outlet at the exit. All fin surfaces and channel walls were set as no-slip and isothermal at 315 K, while the inlet air was 300 K. Only convective heat transfer in the fluid was considered, neglecting conduction in the fin and radiation.

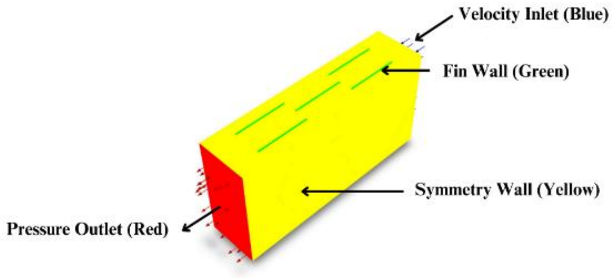

Fig. 2. Computational Domain of OSF with boundary conditions.

Simulations were performed in ANSYS Fluent 2024 under steady-state, incompressible flow conditions using the pressure-based solver. The SIMPLE algorithm handled pressure–velocity coupling. Second-order upwind schemes were used for convective terms and second-order central differencing for diffusion terms. For Re ≤ 1500, laminar flow was assumed, whereas for Re ≥ 2000 the *k–ω* SST turbulence model was employed to capture flow separation and recirculation. Convergence was judged by residuals dropping below 10^{-6} for continuity, momentum, and energy equations.

ANSYS Meshing's patch-conforming method was used to generate an unstructured tetrahedral mesh. Inflation layers with a first-layer height ~10^{-4} m were added to achieve a target $y^+ \leq 1$, depending on fin spacing and Reynolds number.

2.5 Grid Independency and Validation

Mesh independence was checked on the baseline geometry, described in Table 1, at *Re* = 800. The test was conducted for several mesh sizes ranging from ∼100,000 elements to ∼500,000 elements, and the resulting Colburn *j* factor was monitored as a function of mesh size. As shown

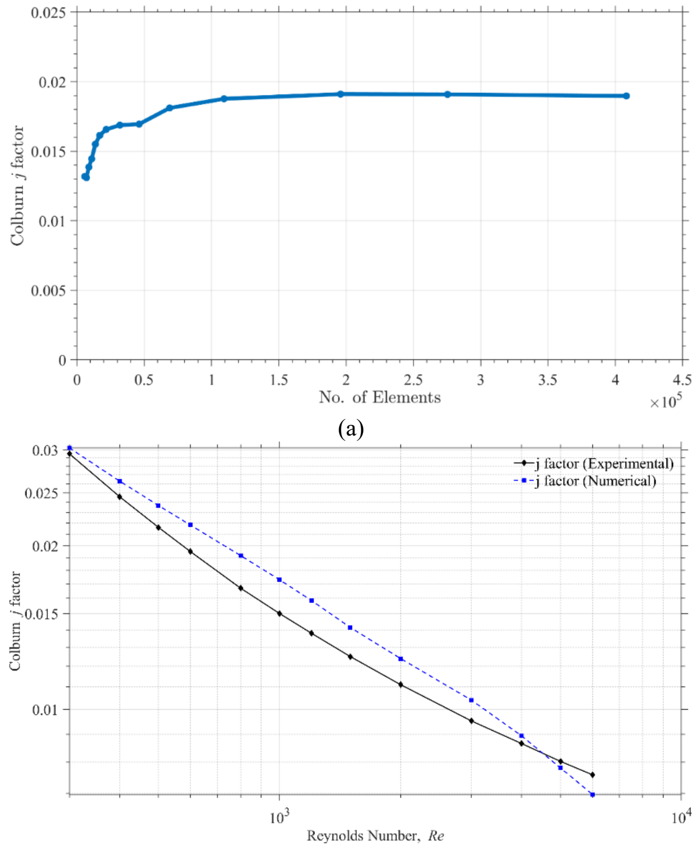

(a)

(b)

Fig. 3. Grid independency test graph for (a) *j* factor vs No. of elements. (b) Comparison between experimental and numerical results for *j* factor for offset strip fins.

in Fig. 3(a), the *j* factor values converge at 304,947 elements, which corresponds to an optimal element size of 0.15 mm. This mesh provided a reliable balance between accuracy and computational efficiency and was adopted for all subsequent simulations in the parametric study. The CFD model was validated against experimental data from Kays and London [2] using the baseline OSF geometry (Table 1) over $300 \leq Re \leq 6000$. Simulated Colburn *j* factors showed good agreement, with deviations within ±8% in the laminar and ±6% in the turbulent regimes (see Fig. 3(b)). Minor discrepancies stem from boundary condition simplifications and surface irregularities, but overall results confirm the model's accuracy.

3 Results and Discussion

The influence of dimensional parameters is interpreted using the dimensionless groups $\alpha = s/h$, $\beta = t/s$, and $\gamma = t/l$, consistent with prior formulations by Manglik and Bergles [4].The parametric study revealed that narrower fin spacing (lower *s*) and thicker fins (higher *t*) consistently led to higher j factors due to enhanced flow acceleration and frequent boundary layer disruption. Increased lance length (higher l) reduced interruption frequency, thereby slightly lowering j values. These trends were consistent across the laminar and turbulent regimes, demonstrating the significant role of geometric configuration in shaping thermal performance.

The correlations modelled using power-law expressions are mentioned below:

$$j = 0.4988 \times Re^{-0.5236} \left(\frac{t}{l}\right)^{0.3860} \left(\frac{s}{b}\right)^{-0.2837} \left(\frac{t}{s}\right)^{-0.4424} ; 300 \leq Re \leq 1500 : laminar\ region \quad (6)$$

$$j = 0.6734 \times Re^{-0.5424} \left(\frac{t}{l}\right)^{0.3830} \left(\frac{s}{b}\right)^{-0.2222} \left(\frac{t}{s}\right)^{-0.4502} ; 1500 \leq Re \leq 6000 : turbulent\ region \quad (7)$$

The correlations yield an $R^2 > 0.95$ in laminar flow and > 0.88 in turbulent flow. These expressions are continuous across flow regimes and explicitly account for geometric parameters. They are also valid for all gases and few liquids with Pr numbers between 0.5 and 15 as mentioned in Manglik and Bergles [4]. A comparison between j factor obtained from the correlation and from the simulation has been shown in Fig.4. Over 95% of the points are observed to be within the 15% bounds.

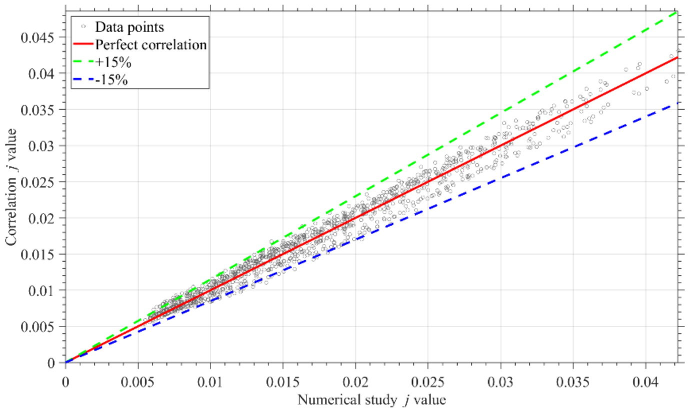

Fig. 4. Comparison between correlation and numerical results for j factor

4 Conclusion

This work presents a comprehensive numerical investigation into the performance of rectangular offset strip fin in compact heat exchangers, resulting in new empirical correlations for the Colburn j factor. The proposed correlations are formulated in terms of Reynolds number, Re, and dimensionless geometric parameters, s/b, t/s, and t/l, and they capture the air-side heat transfer characteristics of OSFs across a wide range of Re in laminar, transition, and turbulent flow regimes. Validation against the classic experimental data of Kays and London [2] confirms that the CFD-derived correlations accurately reproduce established benchmarks for the j factor. Compared to prior correlations in the literature, such as Manglik and Berges [4], the present correlation framework offers improved accuracy while considering the effects of varying flow length and broader applicability by accounting for a wider range of fin geometries and Re. Thus, enabling more effective optimization of OSF configurations compared to earlier models

5 References

1. Voronin, G. I., and Dubrovsky, E. V., 1973, Effective Heat Exchangers, Mashinostroyeniye, Moscow.
2. W.M. Kays, A.L. London, *Compact Heat Exchangers*, 3rd ed., McGraw-Hill, New York, 1984.
3. Wieting, A. R., 1975, "Empirical Correlations for Heat Transfer and Flow Friction Characteristics of Rectangular Offset-Fin Plate-Fin Heat Exchangers," ASME J Heat Transf, 97(3), pp. 488–490. https://doi.org/10.1115/1.3450412
4. Manglik, R. M., and Bergles, A. E., 1995, "Heat Transfer and Pressure Drop Correlations for the Rectangular Offset Strip Fin Compact Heat Exchanger," Exp Therm Fluid Sci, 10(2), pp. 171–180. https://doi.org/10.1016/0894-1777(94)00096-Q
5. Joshi, H. M., and Webb, R. L., 1987, "Heat Transfer and Friction in the Offset Strip-Fin Heat Exchangers," Int J Heat Mass Transf, 30(1), pp. 69–84. https://doi.org/10.1016/0017-9310(87)90061-5
6. Patankar, S. V., and Prakash, C., 1981, "An Analysis of the Effect of Plate Thickness on Laminar Flow and Heat Transfer in Interrupted-Plate Passages," Int J Heat Mass Transf, 24(10), pp. 1801–1810. https://doi.org/10.1016/0017-9310(81)90146-0
7. Dong, J., Chen, J., Chen, Z., and Zhou, Y., 2007, "Air-Side Thermal Hydraulic Performance of Offset Strip Fin Heat Exchangers," Appl Therm Eng, 27(2–3), pp. 306–313. https://doi.org/10.1016/j.applthermaleng.2006.08.005
8. Song, R., Cui, M., and Liu, J., 2017, "A Correlation for Heat Transfer and Flow Friction Characteristics of the Offset Strip Fin Heat Exchanger," Int J Heat Mass Transf, 115(B), pp. 695–705. https://doi.org/10.1016/j.ijheatmasstransfer.2017.08.054
9. Ranganayakulu, C., and Paturu, P., 2011, "Development of Heat Transfer Coefficient and Friction Factor Correlations for Offset Fins Using CFD," Int J Numer Methods Heat Fluid Flow, 21(8), pp. 935–951. https://doi.org/10.1108/09615531111177732
10. Ranganayakulu, C., and Seetharamu, K. N., 2018, Compact Heat Exchangers: Analysis, Design and Optimization Using FEM and CFD Approach, Wiley-ASME Press Series, Wiley, Hoboken, NJ.
11. Kim, M.-S., Lee, J., Yook, S.-J., and Lee, K.-S., 2011, "Correlations and Optimization of a Heat Exchanger with Offset-Strip Fins," Int J Heat Mass Transf, 54(9–10), pp. 2073–2079. https://doi.org/10.1016/j.ijheatmasstransfer.2010.11.056
12. Aujla, G., and Ranganayakulu, C., 2024, "Establishment of Colburn j Factor and Fanning Friction Factor f Correlations for a Compact Heat Exchanger Having Perforated Wavy Fins Using Computational Fluid Dynamics," Int J Heat Fluid Flow, 108, p. 109484. https://doi.org/10.1016/j.ijheatfluidflow.2024.109484
13. Anderson, J. D., 1995, Computational Fluid Dynamics: The Basics with Applications, McGraw-Hill, New York.